

Identification of naphthyridine and quinoline derivatives as potential Nsp16-Nsp10 inhibitors: a pharmacoinformatics study

Bilal J. M. Aldahham, Khattab Al-Khafaji, Mohanad Yakdhan Saleh, Adel Mohamed Abdelhakem, Amer M. Alanazi & Md Ataul Islam

To cite this article: Bilal J. M. Aldahham, Khattab Al-Khafaji, Mohanad Yakdhan Saleh, Adel Mohamed Abdelhakem, Amer M. Alanazi & Md Ataul Islam (2022) Identification of naphthyridine and quinoline derivatives as potential Nsp16-Nsp10 inhibitors: a pharmacoinformatics study, Journal of Biomolecular Structure and Dynamics, 40:9, 3899-3906, DOI: [10.1080/07391102.2020.1851305](https://doi.org/10.1080/07391102.2020.1851305)

To link to this article: <https://doi.org/10.1080/07391102.2020.1851305>



[View supplementary material](#)



Published online: 30 Nov 2020.



[Submit your article to this journal](#)



Article views: 1354



[View related articles](#)





[View Crossmark data](#)



Citing articles: 6 [View citing articles](#)



Identification of naphthyridine and quinoline derivatives as potential Nsp16-Nsp10 inhibitors: a pharmacoinformatics study

Bilal J. M. Aldahham^a, Khattab Al-Khafaji^b, Mohanad Yakdhan Saleh^c , Adel Mohamed Abdelhakem^d, Amer M. Alanazi^e and Md Ataul Islam^{f,g,h} 

^aDepartment of Chemistry, College of Applied Sciences-Hit, University Of Anbar, Anbar, Hit, Iraq; ^bDepartment of Chemistry, College of Arts and Sciences, Gaziantep University, Gaziantep, Turkey; ^cDepartment of Chemistry, College of Education for Pure Science, University of Mosul, Ninawa, Iraq; ^dCollege of Pharmacy, Department of Medicinal Chemistry, Minia University, Mina, Egypt; ^ePharmaceutical Chemistry Department, College of Pharmacy, King Saud University, Riyadh, Saudi Arabia; ^fDivision of Pharmacy and Optometry, School of Health Sciences, Faculty of Biology, Medicine and Health, University of Manchester, Manchester, United Kingdom; ^gSchool of Health Sciences, University of Kwazulu-Natal, Durban, South Africa; ^hDepartment of Chemical Pathology, Faculty of Health Sciences, University of Pretoria and National Health Laboratory Service Tshwane Academic Division, Pretoria, South Africa

Communicated by Ramaswamy H. Sarma

ABSTRACT

This research is a recent effort to explore some new heterocyclic compounds as novel and potential nonstructural protein-16-nonstructural protein-10 (Nsp16-Nsp10) inhibitors for the severe acute respiratory syndrome coronavirus 2 (SARS-CoV-2) inhibition. The SARS-CoV-2 is causative agent of coronavirus disease 2019 (COVID-19) pandemic. A set of 58 molecules belongs to the naphthyridine and quinoline derivatives have been recently synthesized and considered for structure-based virtual screening against Nsp16-Nsp10. Molecular docking was virtually performed to screen for anti-SARS-CoV-2 activity against Nsp16-Nsp10. Fourteen out of fifty-eight compounds were exhibited binding affinity higher than co-crystal bound ligand *s*-adenosylmethionine (SAM) toward Nsp16-Nsp10. Further, the *in silico* pharmacokinetics assessment was carried out and it was found that two molecules possess the acceptable pharmacokinetic profile, hence considered promising Nsp16-Nsp10 inhibitors. The binding interaction analysis was revealed some crucial binding interactions between the final selected two molecules and ligand-binding amino acid residues of Nsp16-Nsp10 protein. In order to explore the characteristics of the protein–ligand complex and how selected small molecules retained inside the receptor cavity in dynamic states, all-atoms conventional molecular dynamics (MD) simulation was performed. Several factors were obtained from the MD simulation trajectory evidently suggested the potentiality of the molecules and stability of the protein–ligand complex. Finally, the binding affinity of both molecules and SAM was explored through the MM-GBSA approach which explained that both molecules possess strong affection towards the Nsp16-Nsp10. Hence, from the pharmacoinformatics assessment, it can be concluded that both heterocyclic compounds might be crucial for SARS-CoV-2 inhibition, subjected to experimental validation.

ARTICLE HISTORY

Received 9 July 2020
Accepted 10 November 2020

KEYWORDS





Naphthyridine and quinoline derivatives; SARS-CoV-2; Nsp16-Nsp10; COVID-19; virtual screening; molecular dynamics simulation


Introduction

The recent mysterious pandemic disease, coronavirus disease 2019 (COVID-19) is caused by the severe acute respiratory syndrome coronavirus 2 (SARS-CoV-2) or 2019 novel coronavirus (2019-nCoV). The SARS-CoV-2 has been added to the list of emerging pathogens seriously affecting human life across the globe. The virus was fulminated from Wuhan, Hubei province, China in December 2019 and growing to be a pandemic illness in the twenty-first century (Zhu et al., 2020). The notified mortality rate in hospitalized patients is about 4% to 11% whereas the overall mortality cases ranged between 2% and 3% (Lipsitch et al., 2020). To date, there is no available therapeutic drug or vaccine to treat or control such pandemic disease. Hence, as of today, not a single

country is left without infections or deaths by the COVID-19. In this uncomfortable situation, the scientific communities across the globe are devoted to finding proper and effective therapeutic agents to treat and control the COVID-19.

The polyproteins are consisting of 16 non-structural proteins (Nsps) (Weiss & Leibowitz, 2011). For RNA stability, protein translation and viral immune escape, the 5'-cap structure of eukaryotic mRNAs is an essential component (Rosas-Lemus et al., 2020). Moreover, 5'-end of viral RNAs copy the cellular mRNA structure. SARS-CoV is consisting of *S*-adenosyl-L-methionine (SAM)-dependent methyltransferases (MTase) which successively methylate the RNA cap at guanosine-N7 and ribose 2'-O positions, catalyzed by Nsp14 N7-MTase and Nsp16 2'-O-MTase, correspondingly (Rosas-Lemus

CONTACT Md Ataul Islam  ataul.islam80@gmail.com  Division of Pharmacy and Optometry, School of Health Sciences, Faculty of Biology, Medicine and Health, University of Manchester, Oxford Road, Manchester, M13 9PL, United Kingdom; Bilal J. M. Aldahham  bilalaldahham@uoanbar.edu.iq  Department of Chemistry, College of Applied Sciences-Hit, University Of Anbar, Hit 31007, Anbar, Iraq.

 Supplemental data for this article can be accessed online at <https://doi.org/10.1080/07391102.2020.1851305>

© 2020 Informa UK Limited, trading as Taylor & Francis Group

et al., 2020). It is also reported that in order to bind the SAM co-factor, the Nsp16 needs the help of Nsp10. It has also been proved that Nsp16 holds the canonical scaffold of MTase and links with Nsp10 at a ratio of 1:1. Moreover, from the structural insight of Nsp16-Nsp10, it has been revealed that Nsp10 may stabilize the SAM-binding pocket and extend the substrate RNA-binding groove of Nsp16 (Rosas-Lemus et al., 2020). The above observations strongly suggested that Nsp16-Nsp10 may be a crucial drug target for highly specific anti-coronavirus drugs in comparison to the viral MTase active site (Rosas-Lemus et al., 2020). Several interesting studies have already been done by considering Nsp16-Nsp10 as an effective drug target for SARS-CoV-2 inhibition (Cavasotto & Di Filippo, 2020; Culetta et al., 2020; Kadioglu et al., 2020; Kandwal & Fayne, 2020; Tazikeh-Lemeski et al., 2020).

Computational screening of approved and new compounds from natural or synthetic sources is one of the excellent and effective approaches to speed up the development process of active agents against SARS CoV-2 pathogenesis (Ojha et al., 2020). It is reported that naphthyridine scaffold containing molecules have shown a wider range of biological activities including antiviral, antimicrobial, anticancer, anti-inflammatory and analgesic (Singh et al., 2017). Similarly, quinoline is belonged to the class of nitrogen heterocyclic compounds and possess anti-malarial, anti-inflammatory, antibacterial, anticancer, anti-microbial, anthelmintic and anti-fungal types of biological activities (Amer et al., 2018; Cocco et al., 2000; Mukherjee et al., 2001; Narender et al., 2005). For instance, the 1,8-naphthyridine and quinoline (Saleh et al., 2020) represent a core for several vital drugs included Gemifloxacin (antimicrobial) (Marchese et al., 2000) and anticonvulsants (Leonard et al., 2002). Beyond above, molecules containing naphthyridine and quinoline scaffolds are also used for dementia (Mekheimer et al., 2007) and cancer therapy (Jiang et al., 2006). Therefore, in the current study, the major efforts were undertaken to identify the novel small molecules that belong to naphthyridine and quinoline derivatives. The molecular docking study was performed on a set of naphthyridine and quinoline derivatives, recently synthesized by our research group (Saleh et al., 2020). Further, *in silico* pharmacokinetics assessment was carried out and finally conventional all-atoms molecular dynamics (MD) simulation was performed. The credential of the work was substantiated by finding two important Nsp16-Nsp10 inhibitors.

Material and methods

Ligand and protein preparation

Structure-based screening of publicly available or in-house databases has become a pivotal drug discovery approach to the pharmaceutical research community. Molecular docking is one of the most widely used structure-based approaches for identifying novel binders by estimating their binding mode and affinity. In the current effort, a set of 58 compounds recently synthesized by our research group (Saleh et al., 2020) were screened through a molecular docking

study against the Nsp16-Nsp10 protein. In the dataset, 10 compounds belong to the 2-chloro-3-formyl quinoline and the remaining belong to the 2-chloro-3-formyl-1,8-Naphthyridine (Saleh et al., 2020). After synthesis, the molecular structures were generated using a molecular drawing tool and subsequently optimized through the density functional theory (DFT) (Becke, 1988) at B3LYP/SDD level implemented in Gaussian09 (Frisch et al., 2016). The two-dimension structure of each molecule is given in Table S1 (Supporting Information). Prior to molecular docking, all the ligands were prepared through the Autodock Tools (ADT) (Morris et al., 2009). One by one each small molecule was taken as ligand input in the ADT followed by hydrogen and Gasteiger charge were added. The torsion root was detected and the number of torsions was set. Finally, each molecule was saved as .pdbqt format for the input of the docking engine. The crystal structures of Nsp16-Nsp10 having PDB ID: 6W4H (Rosas-Lemus et al., 2020) was retrieved from RCSB Protein Data Bank (PDB) (Berman et al., 2000). This structure has been recently crystallized and deposited in the PDB with resolution and *R*-value of 1.8 Å and 0.163, respectively. The selected protein is consisting of two chains, A and B. The A chain is designated as Nsp16 (amino acids range of 6798 to 7096), whereas, B chain signifies the Nsp10 (amino acids range of 4271 to 4386). The co-crystal ligand SAM was extracted and prepared as similar to the ligand preparation. The SAM was considered as a control molecule in the study. The crystal water molecules present in the protein were deleted and missing atoms were repaired. The hydrogens and Gasteiger charge were added. The prepared protein was saved as .pdbqt after assigning the atom type as AD4 (Autodock 4) type.

Molecular docking

Prepared protein and ligands along with SAM were considered for the molecular docking using the AutodockFR (ADFR) program (Ravindranath et al., 2015) with the AutoGridFr (AGFR version 1.0) (Al-Khafaji & Taskin Tok, 2020b; Anderson, 2014). This tool is capable of establishing a configuration file that contains the data for running controlled flexible docking by identifying the residues of the complex's binding site. This enables ligands to reach buried grooves. The docking calculations were run using the default parameters of the ADFR tool (Al-Khafaji & Taskin Tok, 2020a). On successful completion of the docking study, dock score and the binding interaction analyses between protein and ligand were assessed and explored. The validation of the docking protocol is extremely essential and important before starting the experiment. The self-docking method was used to validate the docking protocol in the current study. Initially, the co-crystal ligand was re-generated and docked at the active site where the co-crystal ligand was bound. The best pose was extracted and superimposed on the co-crystal ligand and root-mean-square (RMSD) calculated. It is reported that $RMSD < 2 \text{ \AA}$ validate the docking protocol (Taha et al., 2011). On successful completion of the molecular docking, the binding energy of the docked molecule was compared with the binding energy of SAM.

Molecules having binding energy better than SAM were considered for further assessment. The binding interaction analysis was explored through the online server, Protein–Ligand Interaction Profiler (PLIP) (Salentin et al., 2015).

In silico pharmacokinetic and drug-likeness assessments

Among several assessment criteria, the *in silico* pharmacokinetic (ADME) and drug-likeness analyses are important methods to check the drug-likeness of the molecules obtained from a chemical database. Molecules having docking binding free energy less than SAM were considered for pharmacokinetic analysis. A number of pharmacokinetic and drug-likeness parameters were calculated using the SwissAdme (Daina et al., 2017) included molecular weight (MW), blood-brain barrier (BBB), gastrointestinal absorption (GIA), solubility, synthetic accessibility, Lipinski's rule of five (LoF) and Veber's rule. Molecules satisfied acceptable pharmacokinetic parameters and drug-likeness characteristics were used for further analysis.

MD simulation and binding free energy using MM-GBSA approach

In order to explore the characteristics of final selected molecules and SAM bound with Nsp16-Nsp10 protein molecule in the dynamic state, all-atoms MD simulation for 100 ns time span was performed. The MD simulation study was executed using the Amber20 (Case et al., 2020) installed in Linux platform Dell laptop having 10th Generation Intel Core i9-10885H with NVIDIA® GeForce RTX™ 2070. The topology of Nsp16-Nsp10 was generated using the ff14SB (Maier et al., 2015) force field, while ligand topology was generated through GAFF2 (Träg & Zahn, 2019). Combined protein–ligand systems were solvated using the TIP3P (Mark & Nilsson, 2001) water model and immersed in a truncated octahedron box. The essential number of Na⁺ and Cl⁻ ions were added to neutralize the system. The physiological pH was retained by maintaining the ionic strength of 0.1 M. The simulation was performed using the pmemd.cuda module (Peramo, 2016) of Amber20. In simulation execution, the temperature kept a constant value of 300 K through the Langevin thermostat. The collision frequency was set to 2 ps⁻¹ at 1 atm using a Monte Carlo barostat with volume conversation attempts every 100 fs. The integration step was kept with a 2 fs step. The SHAKE (Andersen, 1983) algorithm was used for the covalent bond constrained associated with hydrogens. In the case of the short-range electrostatic, the threshold was considered to be 8 Å. The particle mesh Ewald method (Petersen, 1995) was considered for the long-range electrostatics. The equilibration of the system was performed for a 10 ns of time span consisting of rounds of NVT and NPT. In order to assess the stability and behavior of the system, several parameters including RMSD of the Nsp16-Nsp10 backbone, RMSD of ligand, root-mean-square fluctuation (RMSF), solvent accessible surface area (SASA), the radius of gyration (RoG) and intermolecular hydrogen bonds were explored

using CPPTRAJ (Roe & Cheatham, 2013) over the full trajectory, taking configuration every 2 ps.

Binding free energy of small molecules obtained from MD simulation trajectory are considered to be more trusted in contrast to the molecular docking binding energy and wisely accepted by the scientific community. The last 10,000 frames of each MD simulation trajectory were used to estimate the binding free energy through the well-known and widely used molecular mechanics-generalized born surface area (MM-GBSA) approach (Genheden & Ryde, 2015). The detailed procedure and expressions can be found in our previous publications (Abdullah et al., 2021; Chikhale et al., 2020).

Results and discussion

Virtual screening

A total of 58 molecules (Table S1, Supporting Information) were docked in the Nsp16-Nsp10 protein molecule. Before molecular docking of the selected dataset, the self-docking method was used to validate the docking protocol. The bound SAM was re-generated and docked to the Nsp16-Nsp10. The best-docked pose of SAM was superimposed to the crystal conformation of SAM. The RMSD of the above superimpose was found to be 1.120 Å which clearly explained the validation of molecular docking protocol (Taha et al., 2011). The superimposed co-crystal and best docked SAM is given in Figure S1 (Supporting Information). The binding energy of SAM was found to be -8.450 Kcal/mol and it was used as a cut-off value for the reduction of chemical space of the molecules. The distribution of binding energy of all molecules including SAM is given in Figure 1.

The binding affinity symbolizes the ability of the molecules to form a stable interaction with the target. The determinant key in virtual screening is to binding affinity such as high negative value indicates the good affinity toward the target, and conversely, molecules having low negative value considered to be inactive. In details analysis, it was found that 14 molecules (Mol2, Mol4, Mol15, Mol16, Mol18, Mol19, Mol35, Mol36, Mol38, Mol43, Mol47, Mol48, Mol52 and Mol57 in Table S1, Supporting Information) found to have higher binding energy (< -8.450 Kcal/mol) in comparison to the binding energy of SAM. Further, the above 14 molecules were used to assess the

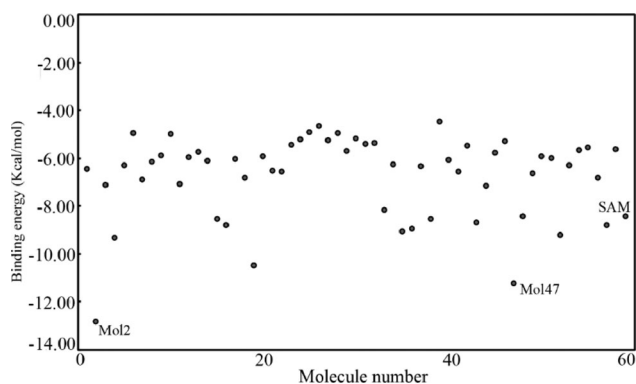


Figure 1. Binding energy distribution of quinoline and naphthyridine derivatives, and SAM.

drug-likeness and pharmacokinetic assessment. It was found that a total of 12 molecules were failed to pass through pharmacokinetics assessment, hence, the remaining two molecules (Mol2 and Mol47 in Table S1, Supporting Information) considered to be promising Nsp16-Nsp10 inhibitors for SARS-CoV-2 inhibition. The two-dimensional representation of the final two molecules and SAM is given in Figure 2.

Binding interaction analysis

The binding interactions between the selected molecules and SAM with Nsp16-Nsp10 were explored through the PLIP. The binding energy of Mol2 and Mol47 was found to be -12.838 and -11.259 Kcal/mol, respectively. The binding interaction profile is given in Figure 3. All three molecules were revealed with some interesting and crucial binding interactions in the form of hydrogen bond (h-bond) and hydrophobic contacts with the catalytic amino acid residues belonging to Nsp16-Nsp10 protein. From Figure 3, it can be seen that Tyr6930 and Asp6931 were formed one h-bond each with Mol2. Phenyl ring present in Mol2 was found crucial to form two hydrophobic interactions with Phe6947. Mol47 was found to form four hydrophobic interactions each with Leu6898, Asp6931, Pro6932 and Phe6947. In addition to the above, Leu6898, Cys6913 and Tyr6930 were revealed critical to establish h-bond interactions with Mol47. Interestingly the SAM was found to form several h-bond interactions with nine different amino acids namely Asn6841, Gly6869, Gly6871, Gly6879, Leu6898, Asn6899, Asp6912, Cys6913 and Tyr6930. No hydrophobic contact was found between SAM and Nsp16. Therefore, the crucial binding interactions

between the final two molecules and Nsp16-Nsp10 will give a strong association that helps to retain stability.

Pharmacokinetics and drug-likeness assessment

The drug-likeness and pharmacokinetics parameters of Mol2 and Mol47 were obtained from the SwissAdme webserver (Daina et al., 2017). The MW of Mol2 and Mol47 was found to be 372.720 and 449.200 g/mol, respectively. The total polar surface area (TPSA) of any molecule less than 140\AA^2 explains the potentiality of the compound. For Mol2 and Mol47, the TPSA was found to be 99.670 and 149.760\AA^2 , respectively. Both molecules were found to be GI absorbable and not permeable to BBB. The synthetic accessibility was found to be 3.08 and 3.92 for Mol2 and Mol47, respectively, which indicates both molecules easy to synthesis. The solubility class explains that both molecules are soluble in nature. A total of 5 rotatable bonds are present in each of Mol2 and Mol47 which indicated that they are not either excessive flexible or rigid. Hence, the above parameters were clearly explained that both molecules possess drug-likeness characteristics.

Molecular dynamics simulation

The steadiness of the complexes between Nsp16-Nsp10 and final small molecules along with SAM was explored through classical MD simulation study for a 100 ns of time span. In order to explore the dynamic nature of the molecules, several parameters include the RMSD, RMSF, RoG, SASA and intermolecular hydrogen bonds were calculated from the MD

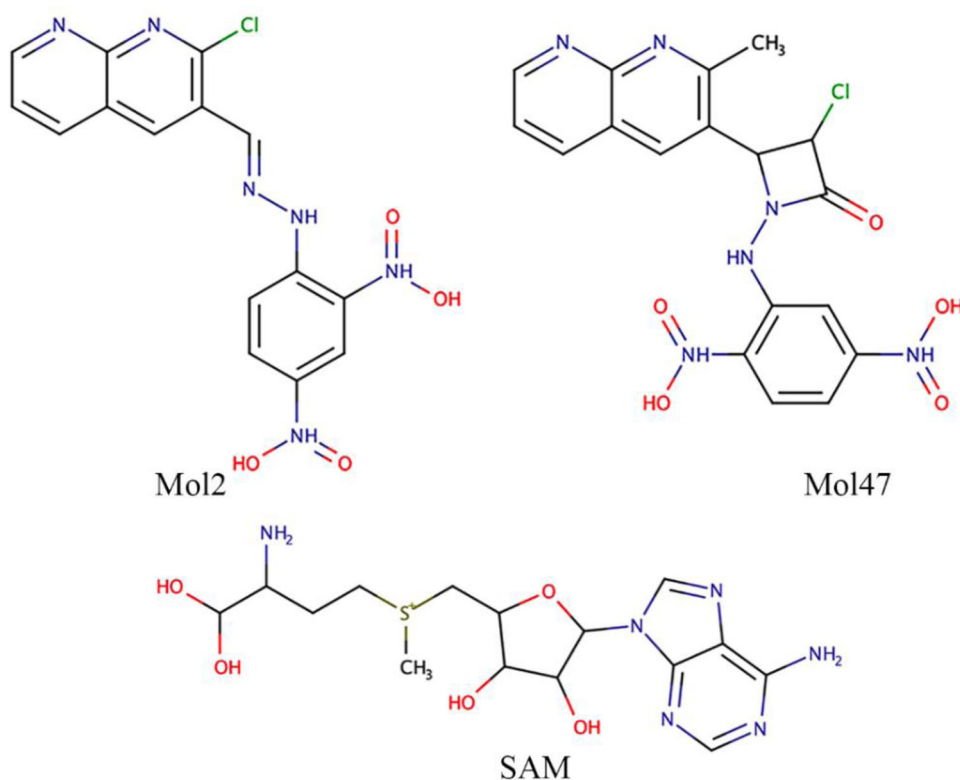


Figure 2. Two-dimensional representation of Mol2, Mol57 and SAM.

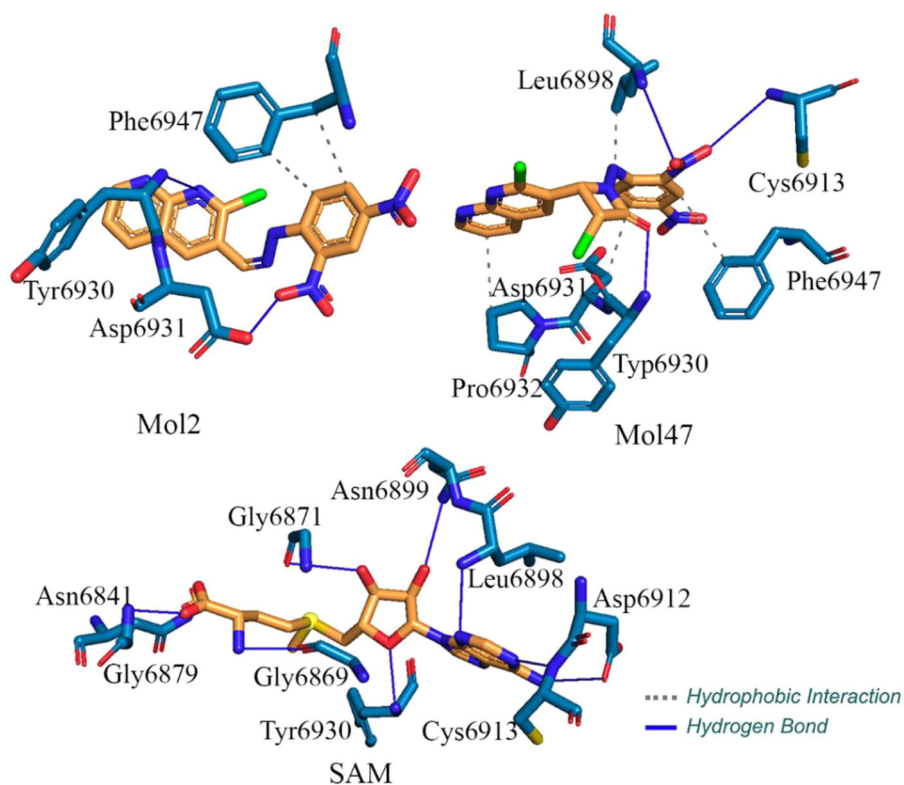


Figure 3. Binding interactions of Mol2, Mol47 and SAM.

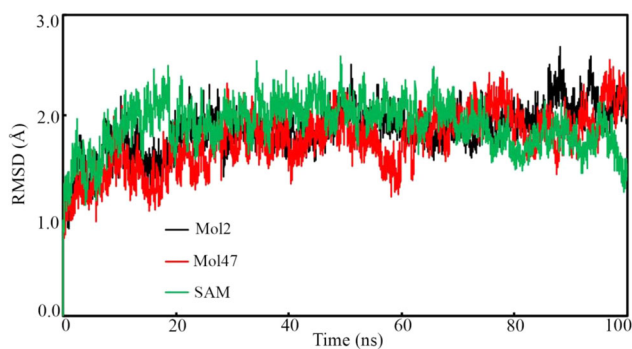


Figure 4. Nsp16-Nsp10 backbone RMSD bound with Mol2, Mol47 and SAM.

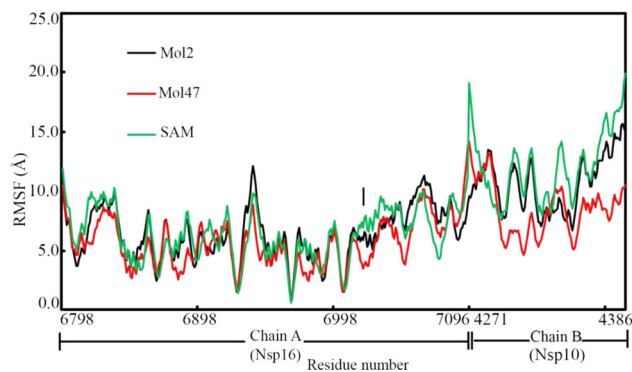


Figure 5. RMSF of amino acid residues of Nsp19-Nsp16.

simulation trajectory of each complex. The average, maximum and minimum value of RMSD, RMSF, RoG and SASA are given in Table 1.

The stability of the protein–ligand complex was assessed through protein backbone RMSD calculated from the MD simulation trajectory. The unfolding of the protein can be indicated by the higher RMSD, whereas low RMSD suggested folding of the protein. Low fluctuation or consistent variation of RMSD defines the system equilibration. Nsp16-Nsp10 backbone RMSD of each frame was calculated and it is given in Figure 4. It can be observed in Figure 4, up to about 20 ns the protein backbone RMSD was increased gradually and afterward achieved the equilibration till the end of the simulation. No abnormal or unusual deviations of the backbone was found. The average RMSD of the backbone can give an impression of the deviation of the protein during MD simulation. Nsp16-Nsp10 backbone average RMSD was found to be 1.851, 1.740 and 1.893 Å when bound to Mol2, Mol47 and

Table 1. Average, maximum and minimum RMSD, ligand-RMSD, RMSF and SASA.

Complex	Mol2	Mol47	SAM
	RMSD (Å)		
Average	1.851	1.740	1.893
Maximum	2.685	2.557	2.585
Minimum	0.000	0.000	0.000
	Ligand-RMSD (Å)		
Average	0.554	1.050	0.464
Maximum	1.740	2.934	1.021
Minimum	0.000	0.000	0.000
	RMSF (Å)		
Average	7.548	6.382	7.952
Maximum	15.674	14.204	19.93
Minimum	0.645	0.562	0.520
	RoG (Å)		
Average	22.760	22.781	22.755
Maximum	23.182	23.223	23.094
Minimum	22.412	22.463	22.344
	SASA (Å ²)		
Average	19,493.850	19,237.660	19,068.410
Maximum	20,653.560	20,454.060	20,100.220
Minimum	18,136.320	18,027.220	17,957.650

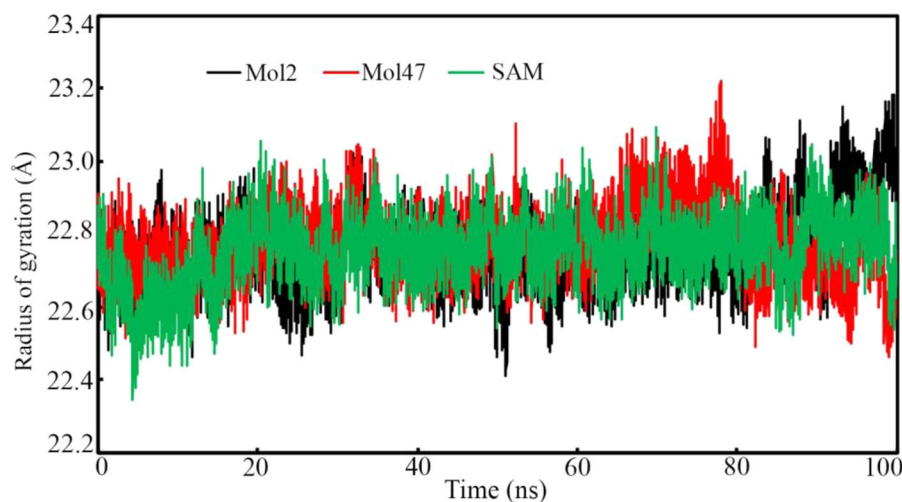


Figure 6. The radius of gyration of Nsp16-Nsp10 bound with Mol2, Mol47 and SAM.

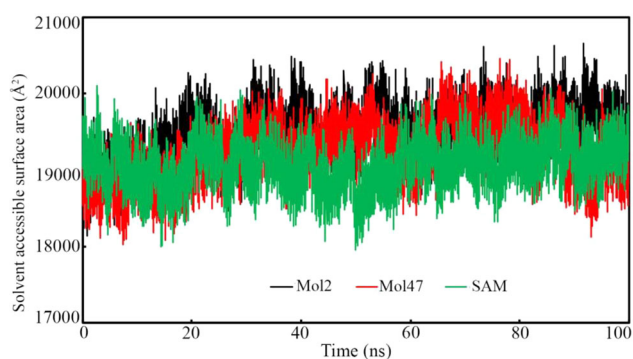


Figure 7. Solvent accessible surface area of Nsp16-Nsp10 bound with Mol2, Mol47 and SAM.

Table 2. Binding free energy of Mol2, Mol47 and SAM.

Molecule	Energy (Kcal/mol)			Standard deviation of ΔG_{bind}
	^a Elec.	^b vdW	ΔG_{bind}	
Mol2	-102.397	-40.962	-45.632	± 3.0766
Mol47	-99.645	-36.126	-41.225	± 4.790
SAM	-87.847	-35.123	-37.262	± 6.050

^aElectrostatic.

^bvan der Waal's.

SAM, respectively. Such low RMSD and consistent variation clearly indicated the stability of the protein–ligand complex during the simulation.

It is important to check the deviation of the ligand with respect to the native conformation during the MD simulation. The ligand-RMSD was calculated and it is given in Figure S2 (Supporting Information). It was observed that Mol2 and SAM was almost remained consistent in the simulation. A little bit deviation of Mol47 was observed that might be due to the orientational change of the molecule. From Table 1, it can be seen that the highest ligand RMSD was found to be 1.740, 2.934 and 1.021 Å for Mol2, Mol47 and SAM, respectively.

Independently the amino acid residues of protein molecule play a critical role to achieve the steadiness of the complex. The fluctuation of the individual amino acid residue can be explored through the RMSF parameter. RMSF of all amino acids belong to the Nsp16-Nsp10 were computed from the MD simulation trajectories and these are given in

Figure 5. Amino acids of Nsp16-Nsp10 were found to deviate almost similar fashion bound with Mol2, Mol47 and SAM. The difference between the maximum and average RMSF can give an idea about fluctuation during the simulation. The above value was found to be 8.126, 7.822 and 11.978 Å when Nsp16-Nsp10 bound with Mol2, Mol47 and SAM, respectively. The above data clearly substantiated the low fluctuation of the amino acid residues in the dynamic states.

The compactness of the Nsp16-Nsp10 bound with Mol2, Mol47 and SAM was explored through the RoG, calculated from the MD simulation trajectory. The RoG of each system was estimated and it is given in Figure 6. Interestingly, all the system stayed compact from start to the end of the simulation. Not a single complex was found with unusual deviation throughout the simulation. The difference between the highest and lowest RoG value of the Nsp16-Nsp10 bound with Mol2, Mol27 and SAM was found to be 0.770, 0.760 and 0.750 Å, respectively. It is quite interesting that proposed molecular systems were retained their compactness as similar to the SAM. Above low deviation and compactness explained the rigidity and stability of the complexes.

The SASA of Nsp16-Nsp10 bound with Mol2, Mol47 and SAM was calculated and monitored over the course of simulations and it is given in Figure 7. This parameter explained the changes in the accessibility of protein to solvent. Not any significant variation of the SASA was observed. From Table 2, it can be observed the difference between the highest and average SASA as 1159.710, 1216.400 and 1031.810 Å² for the Nsp16-Nsp10 bound with Mol2, Mol27 and SAM, respectively. Therefore, overall observations from the parameters obtained using the MD simulation trajectory have clearly explained the stability of the complexes between Nsp16-Nsp10, and Mol2, Mol47 and SAM.

Binding free energy through the MM-GBSA approach

To judge the potentiality of any molecule, the binding free energy (ΔG_{bind}) is one of the important and critical parameters of the small molecule towards the receptor cavity. It is also reported that the ΔG_{bind} calculated using the MM-GBSA

approach can be considered more accurate and acceptable in comparison to the binding energy found in the molecular docking study. The last 10,000 frames of each complex were considered to calculate the ΔG_{bind} of Mol2, Mol47 and SAM, and these are given in Table 2. It can be seen that ΔG_{bind} of Mol2, Mol47 and SAM was found to be -45.632 , -41.225 and -37.262 Kcal/mol, respectively. It is important to note that ΔG_{bind} of proposed molecules was found to be higher than SAM. Hence, Mol2 and Mol47 were shown a better binding affinity towards the Nsp16-Nsp10.

Conclusion

Structure-based virtual screening was performed to explore the promising Nsp16-Nsp10 inhibitors from a set of recently synthesized naphthyridine and quinoline derivatives. The AutodockFR was used to dock all the molecules including co-crystallized SAM. The binding energy of SAM was found to be -8.450 Kcal/mol and considered to be the threshold for the study. Molecules having a higher binding affinity than SAM was considered for *in silico* pharmacokinetic analysis. A total of 14 molecules were found to follow the above criteria. Several pharmacokinetics and drug-likeness parameters were checked. Out of 14 molecules, two compounds were found to follow the pharmacokinetic and drug-likeness assessment and considered to be potential Nsp16-Nsp10 inhibitors. The molecular docking study was revealed a number of important binding interactions between proposed molecules and Nsp16-Nsp10 of SARS-CoV-2. Several parameters were calculated from the MD simulation trajectory clearly explained the potentiality of the molecules. Finally, the MD simulation trajectory of all complexes was considered to find the binding free energy using the MM-GBSA approach. The binding affinity of both selected molecules was obtained higher than SAM, which undoubtedly explained the potentiality of the molecules. Therefore, it can be concluded that both proposed molecules might be crucial chemical scaffolds for Nsp16-Nsp10 of SARS-CoV-2 inhibition as well as starting compounds for synthetic processes to get better inhibitor.

Disclosure statement

No potential conflict of interest was reported by the authors.

Funding

This work was funded by the Researchers Supporting Project Number (RSP-2020/261) King Saud University, Riyadh, Saudi Arabia.

ORCID

Mohanad Yakhdhan Saleh  <http://orcid.org/0000-0003-2320-5167>
Md Ataul Islam  <http://orcid.org/0000-0001-6286-6262>

References

- Abdullah, J. A., Aldahham, B. J. M., Rabeea, M. A., Asmary, F. A., Alhajri, H. M., & Islam, M. A. (2021). Synthesis, characterization and in-silico assessment of novel thiazolidinone derivatives for cyclin-dependent kinases-2 inhibitors. *Journal of Molecular Structure*, 1223, 129311. <https://doi.org/10.1016/j.molstruc.2020.129311>
- Al-Khafaji, K., & Taskin Tok, T. (2020a). Amygdalin as multi-target anti-cancer drug against targets of cell division cycle: Double docking and molecular dynamics simulation. *Journal of Biomolecular Structure and Dynamics*. <https://doi.org/10.1080/07391102.2020.1742792>
- Al-Khafaji, K., & Taskin Tok, T. (2020b). Understanding the mechanism of amygdalin's multifunctional anti-cancer action using computational approach. *Journal of Biomolecular Structure and Dynamics*. <https://doi.org/10.1080/07391102.2020.1736159>
- Amer, A. M., El-Eraky, W. I., & Mahgoub, S. (2018). Synthesis, characterization and antimicrobial activity of some novel quinoline derivatives bearing pyrazole and pyridine moieties. *Egyptian Journal of Chemistry*, 61, 1–8. <https://doi.org/10.21608/ejchem.2018.3941.1345>
- Andersen, H. C. (1983). Rattle: A "velocity" version of the shake algorithm for molecular dynamics calculations. *Journal of Computational Physics*, 52(1), 24–34. [https://doi.org/10.1016/0021-9991\(83\)90014-1](https://doi.org/10.1016/0021-9991(83)90014-1)
- Anderson, S. L. (2014). Dapagliflozin efficacy and safety: A perspective review. *Therapeutic Advances in Drug Safety*, 5(6), 242–254. <https://doi.org/10.1177/2042098614551938>
- Becke, A. D. (1988). Density-functional exchange-energy approximation with correct asymptotic behavior. *Physical Review A, General Physics*, 38(6), 3098–3100. <https://doi.org/10.1103/physrev.38.3098>
- Berman, H. M., Westbrook, J., Feng, Z., Gilliland, G., Bhat, T. N., Weissig, H., Shindyalov, I. N., & Bourne, P. E. (2000). The Protein Data Bank. *Nucleic Acids Research*, 28(1), 235–242. <https://doi.org/10.1093/nar/28.1.235>
- Case, D. A., Belfon, K., Ben-Shalom, I. Y., Brozell, S. R., Cerutti, D. S., Cheatham, T. E., III, Cruzeiro, V. W. D., Darden, T. A., Duke, R. E., Giambasu, G., Gilson, M. K., Gohlke, H., Goetz, A. W., Harris, R., Izadi, S., Izmailov, S. A., Kasavajhala, K., Kovalenko, A., Krasny, R., . . . Kollman, P. A. (2020). *AMBER 2020*. University of California.
- Cavasotto, C. N., & Di Filippo, J. I. (2020). In silico drug repurposing for COVID-19: Targeting SARS-CoV-2 proteins through docking and consensus ranking. *Molecular Informatics*, 39, 2000115. <https://doi.org/10.1002/minf.202000115>
- Chikhale, R. V., Gupta, V. K., Eldesoky, G. E., Wabaidur, S. M., Patil, S. A., & Islam, M. A. (2020). Identification of potential anti-TMPRSS2 natural products through homology modelling, virtual screening and molecular dynamics simulation studies. *Journal of Biomolecular Structure and Dynamics*. <https://doi.org/10.1080/07391102.2020.1798813>
- Cocco, M. T., Congiu, C., & Onnis, V. (2000). Synthesis and antitumour activity of 4-hydroxy-2-pyridone derivatives. *European Journal of Medicinal Chemistry*, 35(5), 545–552. [https://doi.org/10.1016/S0223-5234\(00\)00149-5](https://doi.org/10.1016/S0223-5234(00)00149-5)
- Culletta, G., Gulotta, M. R., Perricone, U., Zappalà, M., Almerico, A. M., & Tutone, M. (2020). Exploring the SARS-CoV-2 proteome in the search of potential inhibitors via structure-based pharmacophore modeling/docking approach. *Computation*, 8(3), 77. <https://doi.org/10.3390/computation8030077>
- Daina, A., Michielin, O., & Zoete, V. (2017). SwissADME: A free web tool to evaluate pharmacokinetics, drug-likeness and medicinal chemistry friendliness of small molecules. *Scientific Reports*, 7, 42717. <https://doi.org/10.1038/srep42717>
- Frisch, M. J., Trucks, G. W., Schlegel, H. B., Scuseria, G. E., Robb, M. A., Cheeseman, J. R., Scalmani, G., Barone, V., Petersson, G. A., Nakatsuji, H., Li, X., Caricato, M., Marenich, A., Bloino, J., Janesko, B. G., Gomperts, R., Mennucci, B., Hratchian, H. P., Ort, J. V., . . . Fox, D. J. (2016). *Gaussian 09, Revision A.02*. Gaussian, Inc.
- Genheden, S., & Ryde, U. (2015). The MM/PBSA and MM/GBSA methods to estimate ligand-binding affinities. *Expert Opinion on Drug Discovery*, 10(5), 449–461. <https://doi.org/10.1517/17460441.2015.1032936>

- Jiang, C., You, Q., Li, Z., & Guo, Q. (2006). Kinesin spindle protein inhibitors as anticancer agents. In *Expert Opinion on Therapeutic Patents*, 16(11), 1517–1532. <https://doi.org/10.1517/13543776.16.11.1517>
- Kadioglu, O., Saeed, M., Greten, H. J., & Efferth, T. (2020). Identification of novel compounds against three targets of SARS CoV2 coronavirus by combined virtual screening and supervised machine learning. *Bull World Health Organ*.
- Kandwal, S., & Fayne, D. (2020). Repurposing drugs for treatment of SARS-CoV-2 infection: Computational design insights into mechanisms of action. *Journal of Biomolecular Structure and Dynamics*. <https://doi.org/10.1080/07391102.2020.1825232>
- Leonard, J. T., Gangadhar, R., Gnanasam, S. K., Ramachandran, S., Saravanan, M., & Sridhar, S. K. (2002). Synthesis and pharmacological activities of 1,8-naphthyridine derivatives. *Biological and Pharmaceutical Bulletin*, 25(6), 798–802. <https://doi.org/10.1248/bpb.25.798>
- Lipsitch, M., Swerdlow, D. L., & Finelli, L. (2020). Defining the epidemiology of Covid-19 — studies needed. *The New England Journal of Medicine*, 382(13), 1194–1196. <https://doi.org/10.1056/NEJMp2002125>
- Maier, J. A., Martinez, C., Kasavajhala, K., Wickstrom, L., Hauser, K. E., & Simmerling, C. (2015). ff14SB: Improving the accuracy of protein side chain and backbone parameters from ff99SB. *Journal of Chemical Theory and Computation*, 11(8), 3696–3713. <https://doi.org/10.1021/acs.jctc.5b00255>
- Marchese, A., Debbia, E. A., & Schito, G. C. (2000). Comparative in vitro potency of gemifloxacin against European respiratory tract pathogens isolated in the Alexander Project. *Journal of Antimicrobial Chemotherapy*, 46(suppl 3), 11–15. <https://doi.org/10.1093/oxfordjournals.jac.a020888>
- Mark, P., & Nilsson, L. (2001). Structure and dynamics of the TIP3P, SPC, and SPC/E water models at 298 K. *Journal of Physical Chemistry A*, 105, 9954–9960. <https://doi.org/10.1021/jp003020w>
- Mekheimer, R. A., Hameed, A. M. A., & Sadek, K. U. (2007). 8-Naphthyridines II: Synthesis of novel polyfunctionally substituted 1,8-naphthyridinones and their degradation to 6-aminopyridones. *Arkivoc*, 2007(13), 269–281. <https://doi.org/10.3998/ark.5550190.0008.d30>
- Morris, G. M., Goodsell, D. S., Pique, M. E., Lindstrom, W., Lindy Huey, R., Forli, S., Hart, W., Halliday, E., Belew, S., & Olson, R. A. J. (2009). Autodock4 and AutoDockTools4: Automated docking with selective receptor flexibility. *Journal of Computational Chemistry*, 30(16), 2785–2791. <https://doi.org/10.1002/jcc.21256>
- Mukherjee, S., Kumar, V., Prasad, A. K., Raj, H. G., Bracke, M. E., Olsen, C. E., Jain, S. C., & Parmar, V. S. (2001). Synthetic and biological activity evaluation studies on novel 1,3-diarylpropenones. *Bioorganic and Medicinal Chemistry*, 9, 337–345. [https://doi.org/10.1016/S0968-0896\(00\)00249-2](https://doi.org/10.1016/S0968-0896(00)00249-2)
- Narender, T., Shweta, Tanvir, K., Srinivasa Rao, M., Srivastava, K., & Puri, S. K. (2005). Prenylated chalcones isolated from *Crotalaria* genus inhibits in vitro growth of the human malaria parasite *Plasmodium falciparum*. *Bioorganic and Medicinal Chemistry Letters*, 15, 2453–2455. <https://doi.org/10.1016/j.bmcl.2005.03.081>
- Ojha, P. K., Kar, S., Krishna, J. G., Roy, K., & Leszczynski, J. (2020). Therapeutics for COVID-19: From computation to practices—Where we are, where we are heading to. *Molecular Diversity*. <https://doi.org/10.1007/s11030-020-10134-x>
- Peramo, A. (2016). Solvated and generalised Born calculations differences using GPU CUDA and multi-CPU simulations of an antifreeze protein with AMBER. *Molecular Simulation*, 42(15), 1263–1273. <https://doi.org/10.1080/08927022.2016.1183000>
- Petersen, H. G. (1995). Accuracy and efficiency of the particle mesh Ewald method. *The Journal of Chemical Physics*, 103(9), 3668–3679. <https://doi.org/10.1063/1.470043>
- Ravindranath, P. A., Forli, S., Goodsell, D. S., Olson, A. J., & Sanner, M. F. (2015). AutoDockFR: Advances in protein-ligand docking with explicitly specified binding site flexibility. *PLoS Computational Biology*, 11(12), e1004586. <https://doi.org/10.1371/journal.pcbi.1004586>
- Roe, D. R., & Cheatham, T. E. (2013). PTRAJ and CPPTRAJ: Software for processing and analysis of molecular dynamics trajectory data. *Journal of Chemical Theory and Computation*, 9(7), 3084–3095. <https://doi.org/10.1021/ct400341p>
- Rosas-Lemus, M., Minasov, G., Shuvalova, L., Inniss, N., Kiryukhina, O., Wiersum, G., Kim, Y., Jedrzejczak, R., Maltseva, N., Endres, M., Jaroszewski, L., Godzik, A., Joachimiak, A., & Satchell, K. (2020). The crystal structure of nsp10-nsp16 heterodimer from SARS-CoV-2 in complex with S-adenosylmethionine. *BioRxiv: The Preprint Server for Biology*. <https://doi.org/10.1101/2020.04.17.047498>
- Saleh, M., Ayoub, A., & Hammady, A. (2020). Synthesis biological studies of some new heterocyclic compound derived from 2-chloro-3-formyl quinoline and 4-(benzyl sulfonyl) acetophenone. *Egyptian Journal of Chemistry*. <https://doi.org/10.21608/ejchem.2020.26354.2535>
- Salentin, S., Schreiber, S., Haupt, V. J., Adasme, M. F., & Schroeder, M. (2015). PLIP: Fully automated protein-ligand interaction profiler. *Nucleic Acids Research*, 43(W1), W443–W447. <https://doi.org/10.1093/nar/gkv315>
- Singh, I. P., Kumar, S., & Gupta, S. (2017). Naphthyridines with antiviral activity - a review. *Medicinal Chemistry*, 13(5), 430–438. <https://doi.org/10.2174/1573406412666161228112127>
- Taha, M. O., Habash, M., Al-Hadidi, Z., Al-Bakri, A., Younis, K., & Sisan, S. (2011). Docking-based comparative intermolecular contacts analysis as new 3-D QSAR concept for validating docking studies and in silico screening: NMT and GP inhibitors as case studies. *Journal of Chemical Information and Modeling*, 51(3), 647–669. <https://doi.org/10.1021/ci100368t>
- Tazikheh-Lemeski, E., Moradi, S., Raoufi, R., Shahlaei, M., Janlou, M. A. M., & Zolghadri, S. (2020). Targeting SARS-COV-2 non-structural protein 16: A virtual drug repurposing study. *Journal of Biomolecular Structure and Dynamics*. <https://doi.org/10.1080/07391102.2020.1779133>
- Träg, J., & Zahn, D. (2019). Improved GAFF2 parameters for fluorinated alkanes and mixed hydro- and fluorocarbons. *Journal of Molecular Modeling*, 25(2), 39. <https://doi.org/10.1007/s00894-018-3911-5>
- Weiss, S. R., & Leibowitz, J. L. (2011). Coronavirus pathogenesis. In *Advances in virus research*. Elsevier. <https://doi.org/10.1016/B978-0-12-385885-6.00009-2>
- Zhu, N., Zhang, D., Wang, W., Li, X., Yang, B., Song, J., Zhao, X., Huang, B., Shi, W., Lu, R., Niu, P., Zhan, F., Ma, X., Wang, D., Xu, W., Wu, G., Gao, G. F., & Tan, W. (2020). A novel coronavirus from patients with pneumonia in China, 2019. *The New England Journal of Medicine*, 382(8), 727–733. <https://doi.org/10.1056/NEJMoa2001017>